Nano Energy 96 (2022) 107063

Contents lists available at ScienceDirect

Nano Energy

journal homepage: www.elsevier.com/locate/nanoen

Communication

A triboelectric-inductive hybrid tactile sensor for highly accurate object recognition

Ning Li [a,b,1], Zhuhui Yin [a,1], Weiguan Zhang [a,b], Chenyang Xing [a], Taijiang Peng [b], Bo Meng [a,*], Jun Yang [c], Zhengchun Peng [a,*]

[a] Key Laboratory of Optoelectronic Devices and Systems of Ministry of Education and Guangdong Province, College of Physics and Optoelectronic Engineering, Shenzhen University, Shenzhen 518060, P.R. China
[b] College of Mechatronics and Control Engineering, Shenzhen University, Shenzhen 518060, P.R. China
[c] Shenzhen Institute for Advanced Study, University of Electronic Science and Technology of China, Shenzhen 518000, P.R. China

ARTICLE INFO

Keywords:
Hybrid tactile sensor
Triboelectric active sensing
Inductance transducer
Machine learning
Object recognition

ABSTRACT

Tactile sensors can enable a robotic manipulator to identify the object in contact. However, due to the dynamics and diversity of target objects, as well as the complexity of real environment, accurate recognition of objects by existing tactile sensors has been very challenging. This paper proposes a hybrid tactile sensor that integrates a triboelectric active sensing unit with an electromagnetic inductance transducer. The triboelectric signal relates strongly to the specific charge condition of the surface material of a target object, while the inductive signal manifests the electromagnetic characteristics at a certain depth inside the object. With the help of machine learning, the triboelectric signals and inductive signals can be used for object identification. We demonstrate a robotic gripper with random operation settings can recognize eight different fruits with an accuracy as high as 98.75%. Furthermore, the hybrid sensor can recognize objects packaged in different ways. The recognition accuracy of four different fruits in three different packages can reach 95.93%. This study demonstrates the potential of hybrid tactile sensor to improve the artificial intelligence of robots, in particular their ability to distinguish objects in complex settings and sorting them effectively.

1. Introduction

Artificial general intelligence (AGI) demands real-time information acquisition and data analysis. As such, a large number of sensors need to be deployed under the framework of internet of things (IoT) [1]. The ability to recognize objects is the technical basis for robots to make decisions such as how to properly handle them [2]. Visual recognition is the main method used by robots to transform physical objects into digital models [3]. However, the accuracy of object recognition using visual technology is limited by the interference of light and angles, resolution of image acquisition, and object occlusion. [4] In particular, distinguishing transparent objects by vision is extremely difficult. Furthermore, visual technology cannot evaluate some of important characteristics of an object such as its rigidity and the type of material it is made of.

Object recognition based on haptic technology has been widely studied to supplement the visual technology. A pressure sensor array is an effective tool to characterize the surface roughness of a target object and perceive the slip sensation as a robotic gripper transfers the object [5]. However, it is difficult to decouple the interference of the shape of an object from the sliding error of the robotic gripper, which limits the application of this technology in robotics. Sundaram et al. proposed a data glove composed of 548 resistance sensors in a dense matrix to obtain more detailed characteristics of an object such as the contour and the rigidity of the object, in order to establish suitable gripping strategy for a robotic manipulator to handle different objects [6]. However, analyzing massive data collected by a large number of sensors poses a major challenge to system robustness.

The phenomenon of triboelectrification has been explored for energy harvesting and active sensing purposes [7–10]. Research on triboelectric nanogenerators (TENG) has been growing very fast in the past few years [11–19]. Among the various types of TENGs, single electrode triboelectric nanogenerator (STENG) adopts an open surface structure [20,21]. The output signal of the STENG is determined by the specific charge

* Corresponding authors.
E-mail addresses: bomeng@szu.edu.cn (B. Meng), zcpeng@szu.edu.cn (Z. Peng).
[1] These authors contributed equally to this work

https://doi.org/10.1016/j.nanoen.2022.107063
Received 12 December 2021; Received in revised form 28 January 2022; Accepted 14 February 2022
Available online 16 February 2022

interaction between the triboelectric layer and the target object [20–22]. Therefore, through simple contact-separation mode STENG can extract the electrical properties of the surface material of an object. Zhu et al. developed a data glove with 16 triboelectric sensors to recognize objects with a high accuracy of 96% [23]. Wen et al. successfully used 10 triboelectric sensors for gesture identification with an accuracy of 95% [24]. Lee group at National University of Singapore combined the triboelectric characteristic and contour feature to obtain unique characteristic tag of the object. They also discussed the machine learning algorithms used for object recognition, and future autonomous IoT technology to be used in the field of sorting robotics [25,26].

Due to the diverse tasks of sorting robotics, the target objects such as fruits with varying levels of ripeness have very different shape and rigidity. Triboelectric signal only accounts for the specific charge interaction of the object's surface, it cannot be used to identify other characteristics of the object such as texture, temperature, the property of the material inside the object, etc. In addition, when a sorting robot equipped with triboelectric sensors grips an object, the triboelectric signal is not only attributed to the gain or loss of specific charges at the interface, but also to the approaching speed of the contact as well as the contact area [27,28]. With densely distributed mechanosensitive receptors, human skin can perceive multiple physical stimuli exerted at the same location. Fully replicating this behavior in artificial sensors is still an unresolved problem [29], although some progress has been made in constructing two or more types of sensors on the same spot [27,30,31]. This is mainly due to the limited integration of multi-parameter tactile sensors with high resolution arrays in a single sensory locus.

The electromagnetic induction of an object is one of its inherent characteristics and is related to factors such as the shape, conductivity, and water content of the object. The electromagnetic characteristics of an object can be conveniently measured with inductance sensors. Inductance sensors have a large detection depth, which can overcome the limitations of triboelectric sensors that can only recognize the surface material properties of an object. In this paper, we propose a dual-mode tactile sensor by integrating a triboelectric sensor array with an inductance sensor in the same location. By feeding the triboelectric signals and induction signals of different objects to machine learning models, we aim to develop a strategy that can enable robotic grippers to identify a variety of objects with high accuracy.

2. Results and discussions

2.1. Design and fabrication of the hybrid sensor

Schematics of the proposed hybrid sensor are presented in Fig. 1a. Structurally, the hybrid sensor consists of two units. A single-electrode triboelectric sensor composed of a polyvinylidene fluoride (PVDF) triboelectric layer and a copper electrode acquires the surface charge interaction when contacting a target. A planar inductance sensor composed of constantan coils measures the electromagnetic induction of a target. These two sensors are arranged in concentric circles and distributed in the same plane to ensure the synchronization of the two signals. A shield ring with a common connection to ground for both sensors is used to avoid mutual interference, such that the two sensing units can operate independently.

The working mechanisms of the triboelectric sensor is illustrated in Fig. 1b. When external stimuli are provided by triboelectrification or electrostatic induction, the electrical potential between the electrode and the ground increases, driving electrons to flow through external resistors to the electrode, thereby generating a positive voltage, as shown in Fig. 1c. Similarly, when the stimuli are removed, the electrical potential will change back to its original state and the induced negative

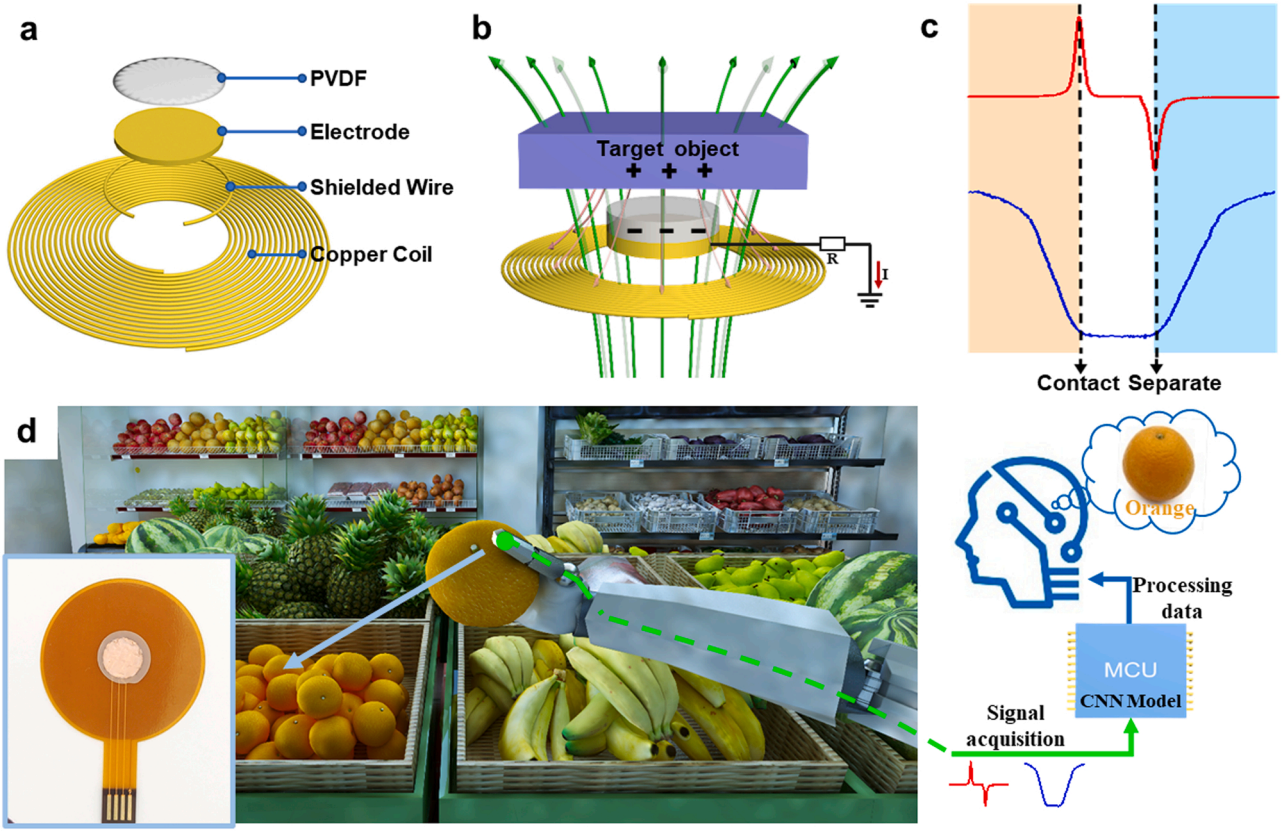

Fig. 1. Schematic illustration of the dual-mode tactile sensor. a) Design of the dual-mode tactile sensor. b) Working mechanism of the dual-mode tactile sensor. c) Typical signals from the dual-mode tactile sensor when touching an object. d) Concept of object recognition by a robotic gripper equipped with the dual-mode tactile sensor.

charges on the electrode will flow back to the ground, generating a negative voltage. The PVDF film is laser engraved to form ring structure that mimics the surface texture of a human finger. The microstructures can effectively improve the amplitude of the triboelectrification (Fig. S1). The working mechanisms of the inductance sensor is also illustrated in Fig. 1b. Alternating current flowing through a set of concentric coils can generate alternating electromagnetic field, which will induce an internal current loop inside the object that is close to the coils, resulting in mutual inductance. The intensity of mutual inductance increases as the inductance coil approaching the object, and reaches a maximum value when the sensor contacts the object (Fig. 1c).

Fig. 1d shows the objective of this work, i.e., using the proposed hybrid sensor to help a robot to identify a variety of fruits. By adopting machine learning models to fuse the dual-mode sensing information, an advanced identification system can be constructed, which measures not only the surface property of the target object, but also the characteristic of the inner content of the object. This identification system is highly demanded by future sorting robots in supermarket.

2.2. Characterization of the hybrid sensor

To analyze the performance of the hybrid sensor, we attach the hybrid sensor to the pressure head of a universal material test instrument (Fig. S2a, b). A piece of copper foil is tiled on the base of the instrument as the target object. The universal material test instrument drives the sensor to press on the copper foil. The test instrument can produce various types of mechanical strokes with programable force and frequency. Fig. 2a presents the result of 1000 repeated tests with a load of 20 N at a frequency of 1 Hz. It reveals stable response of the hybrid sensor to repeated excitations. Which shows stable response of the hybrid sensor to repeated excitations. Zooming in the data reveals the synchronicity of the dual mode signals.

Fig. 2b shows that the output voltage of the triboelectric sensor increases slightly with the applied pressure. The two opposite peaks represent the contact and separation processes, respectively. When the contact pressure is set to 5 N (12.5 kpa), the peak value of the triboelectric voltage is 1.31 V. When the contact pressure increases to 35 N (87.5 kpa), the peak value of the triboelectric voltage is 1.68 V. The variation of contact pressure could affect the triboelectric signal, but it's not a major factor. However, when the inductive sensor approaches to the target object with different contact pressures, the output signals exhibit little differences (Fig. 2c), indicating that inductance is insensitive to contact pressure.

When driving the hybrid sensor to press on the copper foil, the pressure head of the universal material test instrument was programmed to move with the same displacement in the form of a triangular wave motion at different frequencies. The triboelectric sensor outputs a series of steady and continuous V-T curves. With different frequencies, the pressure head drives the sensor to contact the copper foil at different speeds. The amplitude of the triboelectric signals increases significantly with the contact speed (Fig. 2d). The output of the triboelectric sensor is enhanced to 2.12 V when operating at a velocity of 20 mm/s (2.5 Hz). In comparison, the amplitude of the inductive signals is not affected by contact speed (Fig. 2e).

When a robotic manipulator grasps a soft object, the contact position would sink into the target object. To simulate this scenario, we placed an elastomer gasket made of Ecoflex gel (M1) underneath the copper foil. As shown in Fig. S2c, the pressure head drives the sensor with different distances from the starting position of 10 cm above the copper foil. We set the position at which the sensor just touches the copper foil as the zero point. The contact distances were set in the range of $-3 - 2$ mm, where a negative value indicates that the sensor not only contacts with the object, but also compresses into it. As shown in Fig. 2f, faint triboelectric signal can be observed when the contact distance falls in the range from 0.25 to 0.75 mm. This result can be attributed to the accumulation of induced charges when the triboelectric sensor is close to the target. As the sensor touches the target, the peak voltage of the triboelectric signal increase dramatically, and it correlates strongly with the indentation depth, i.e., it increases with an increasing indentation depth, which is attributed to the increase of contact area as the sensor compresses into the soft object. When the contact distance reaches -2.5 mm, the amplitude of triboelectric signal states to saturate.

The peak value of the inductance sensor increases as the ingot head approaches to the copper foil (Fig. 2g). The main reason is that the distance to the target object and the plane inductance are closely related to the mutual inductance of the electromagnetic field. However, with an increase in the indentation depth, the peak value of the inductance sensor remains relatively stable.

We used Ecoflex with different models to prepare elastic gaskets with different order of hardness (the order of hardness of the five samples is: M5 > M4 > M3 > M2 > M1), and then covered them with copper foil (Table S1). The indenter was set to press on the five samples at the same speed with the same displacement stroke (10 cm to -1 mm). The signals are presented in Fig. 2h and i. The output signal of the triboelectric sensor related strongly to the hardness of the target object, while the output signal of the inductance sensor is independent of the hardness.

We installed the hybrid sensor on a robotic gripper and set the robot to grasp a fruit and then release it (Fig. S3). The instruments for data acquisition, data processing and identification are shown in Fig. S4. To eliminate the effects of grasping movements, we need to ensure that the gripper makes tight contact with the fruits. The signals from the dual-mode sensor as the robotic gripper handles different fruits are shown in Fig. 3. First, we set the robot to grip the same spot on the surface of a fruit for three times. Within the triple touches at the same spot on the surface of the same fruit, the waveforms of both triboelectric and inductive signals are similar, indicating good repeatability of the hybrid sensor. The characteristics of the dual-mode signals differ significantly for different fruits (Fig. 3a), indicating that both signals can be used to extract the inherent properties of target fruits. In addition, the fusion of the two signals would lead to better perception and more complete knowledge of the target. In fact, it takes several grasping cycles for the amplitude of the triboelectric signals to reach stable values (Fig. S5).

Fig. S6 shows the volume and shape of the fruit have influence on the mutual inductance. However, it is not the inductance signal alone that we use to identify the fruit. Instead, we complement the inductance signal with the triboelectric signal of the same fruit. Which will limit the effect of the inductance variation from the size and shape of the same fruit. In order to explore the relationship between the induction and the conductivity of the fruits, we cut 8 fruits into 8 slices of similar size and repeated the above experiment. Fig. 3b indicates that the inductance of different fruit slices is strongly correlated with the conductivity of the fruits. This result aligns with the electromagnetic theory that the mutual inductance is a strong function of the electrical conduction of the target object. As the electrical conductivity of the object increases, the mutual inductance increases. Fig. S7 indicates when the inductance sensor approaches to metals such as copper, iron and aluminum, the induction is very strong and has different characteristics for different metals. However, there's no obvious induction to low dielectric materials such as glass, wood and Nylon. In this case, only the triboelectric signals contribute to the machine learning outcome. In comparison, the induction signals from fruits lie in between insulators and metals.

In practical applications, the grasp and release actions of a robot gripper involve considerable randomness. For instance, the position of the contact between a mechanical finger and object also changes during multiple grasping motions. In addition, with the same gripping force the contact area varies with the rigidity of the object. Furthermore, the signal of the triboelectric sensor is affected by the grasping speed of the gripper. To simulate these scenarios, we set different grasping postures for the gripper, and randomly adjusted the orientation of the target fruits so that the robot grips different spots on the surface each time. These random gripping settings can circumvent the influence of the aforementioned unsaturated amplitude of the triboelectric signals. Under

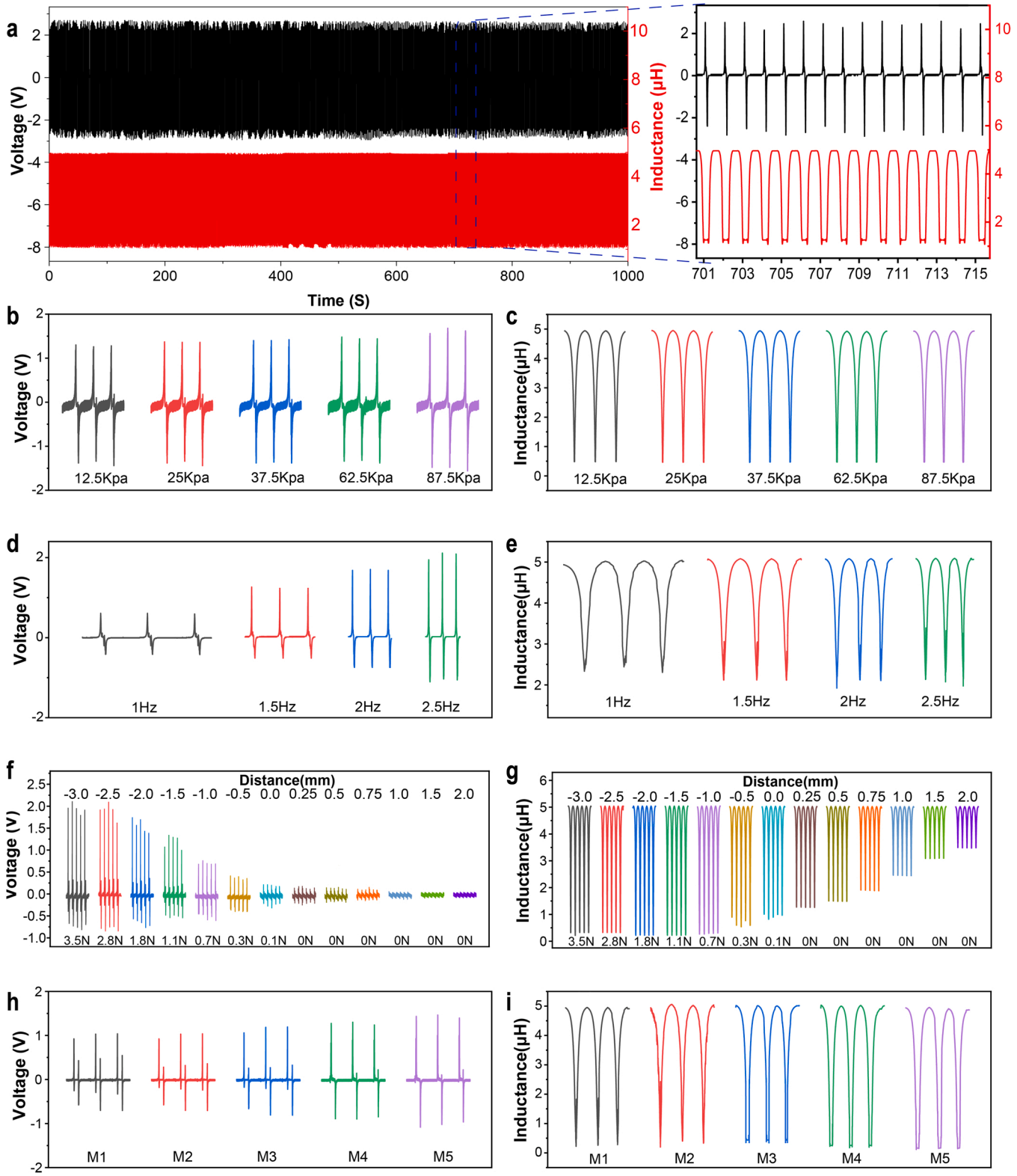

Fig. 2. Electric characterization of the hybrid sensor under different test conditions. a) Bi-channel output of triboelectric and inductive signals from repeated contact of an object. b) Triboelectric signals and c) inductive signals under different contact forces. d) Triboelectric signals and e) inductive signals under different contact frequencies. f, g) The response of the hybrid sensor as it approaches to a soft object with different contact distances defined by the stopping point of the motor. h) Triboelectric signals and i) inductive signals from touching five kinds of Ecoflex samples. (the order of hardness of the five samples is: M5 > M4 > M3 > M2 > M1).

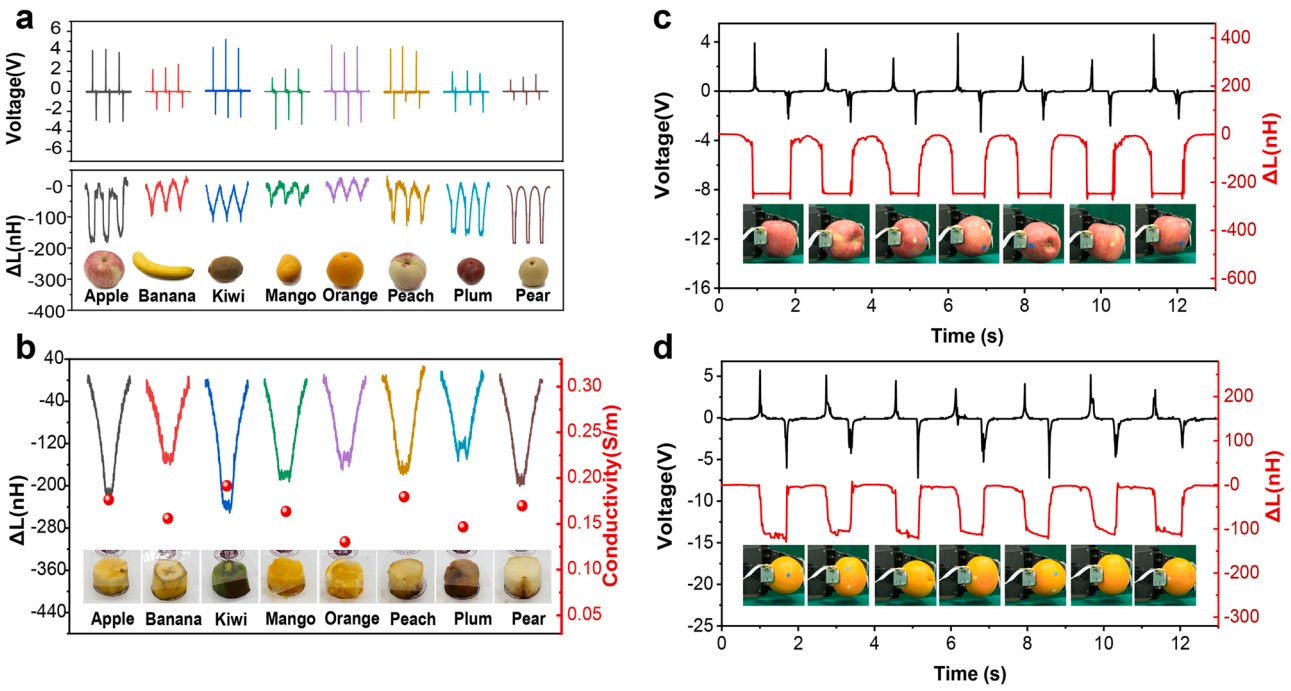

Fig. 3. a) The sensing signals from the dual-mode sensor as it contacts 8 fruits. b) Inductance signals from the 8 fruit cylinders of similar size, along with the corresponding conductivity of the 8 fruits. c, d) The sensing signals from the dual-mode sensor as it touches different spots on the surface of a fruit.

these test conditions, we collected data on different fruits. The dual-mode signals from two of them, i.e., apple and orange, are presented in Fig. 3c, d. With different grip conditions and contact positions, the triboelectric signal exhibits clear fluctuations, whereas the inductive signal is less affected. This finding indicates that it is necessary to acquire various inherent features of objects simultaneously and

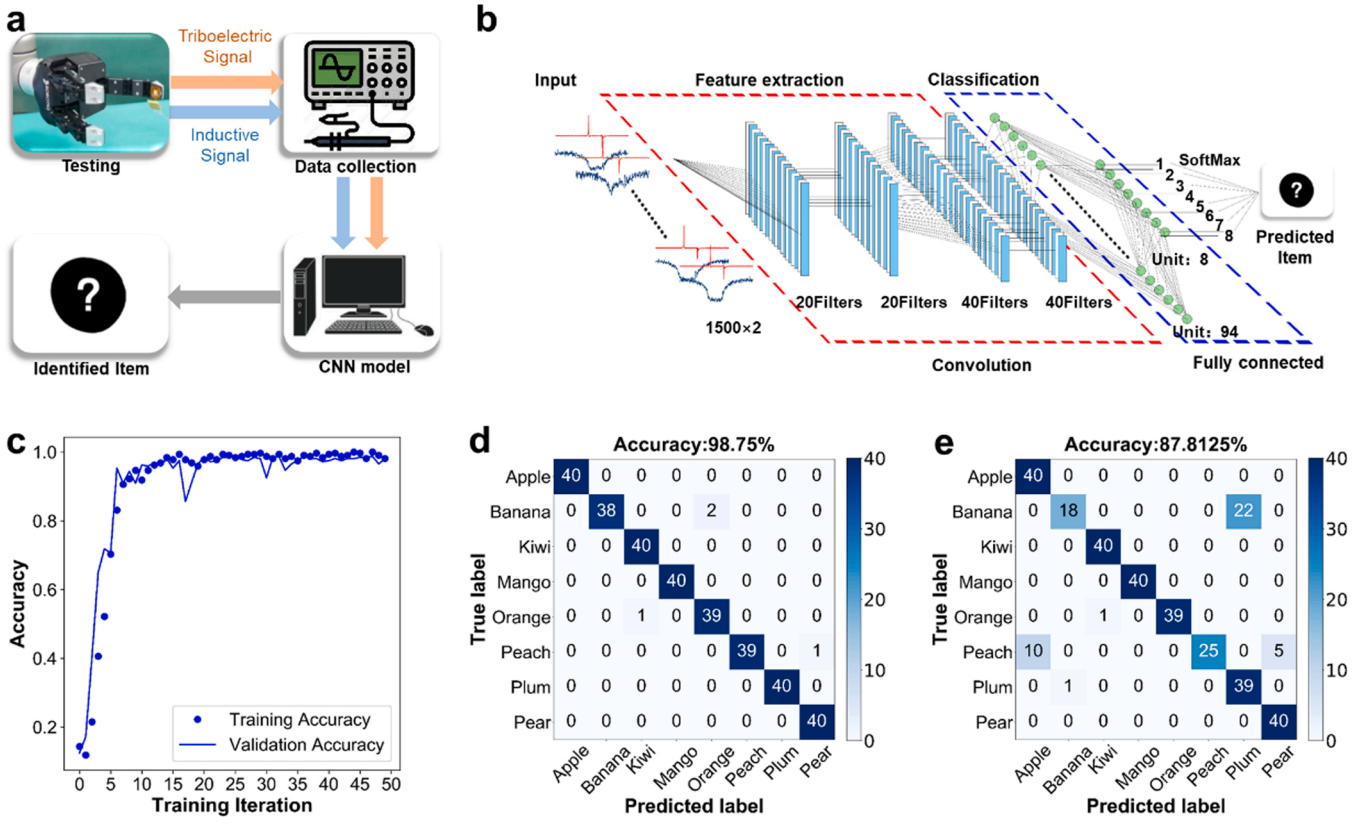

Fig. 4. Object recognition by a robotic gripper equipped with a dual-mode hybrid sensor. a) Schematic diagram of the process flows from dual-mode sensing to data processing with machine learning. b) The detailed framework of the 1D-CNN model. c) The relationship between identification accuracy and the number of epochs. d, e) Confusion matrixs of object recognition derived from two CNN models using the database of dual-mode signals and triboelectric signals alone, respectively.

independently in practical applications. As such, these two sensors are very complementary, making the hybrid sensor promising for accurate object recognition.

2.3. Convolutional neural network for object recognition

Incorporating neural networks and deep learning with tactile sensors can create better haptic perception and more accurate object recognition. The approach has also been proven effective in solving classification problems without involving in an explicit model [32].

Machine learning is an effective approach to dealing with classification problems with complicated input signals. It can extract characteristic features from seemly irrelated data set. [33,38] Fig. 4a shows a complete machine learning process from signal acquisition to data processing. In this study, we implemented a one-dimensional convolutional neural network (1D-CNN) for the dual-mode signal processing and data analysis. The convolutional neural network consists of four convolution layers, two pooling layers, and two fully connected layers (Fig. 4b). The convolution layer can extract the characteristics of the signal for better analysis of the data. Eight fruits shown in Fig. 3a are selected as target objects. Sensing signals were collected as a robot equipped with the hybrid sensor gripped these fruits for 200 times. To simulate the practical gripping scenarios, three different gripping forces and three different gripping speeds were programmed. The 200 pieces of data were randomly shuffled to construct the training set and the test set. The two groups were split at a ratio of 8:2 (training: 160 samples, testing: 40 samples).

We first set the number of convolutional layers in the model to 2 and determined the optimal number of neurons in the hidden layer by changing the number of convolutional layers. As shown in Fig. S8, the accuracy increases with an increase in the number of convolutional layers. When the number of neurons is greater than four, accuracy saturation is achieved and an overfitting phenomenon appears. Therefore, the number of convolutional layers was taken as 4. Referring to several popular CNN models [34–36], it is demonstrated that the pyramid construction of channel is efficient. As to CNN model, the numbers of channel in each convolutional layer were set to 20, 20, 40, and 40 (Fig. 4b). Similarly, we studied the training iteration and determined the optimal numbers. Fig. 4c reveals that when the training iteration reaches 20, the accuracy tends to converge and fluctuates in a narrow range (From 94.6875% to 99.6875%). To prevent overfitting [37], we set the number of cycles to 25.

By combining triboelectric and inductive signals, the recognition accuracy of 8 different fruits reaches 98.75% (Fig. 4d), indicating that the trained CNN model has a high positive predictive value and true positive rate for object recognition. It takes about 0.778 s for the trained model to recognize each fruit. Fig. 4e presents the identification results when using the triboelectric signals alone. The identification accuracy of the triboelectric sensor is only 87.81%. This is because the signal of a single mode of triboelectric sensor is coupled with a variety of disturbances, while the dual-mode signals can effectively decouple the interferences caused by the differences in the contact dynamics between the gripper and the targets. Even for the same type of fruit, there are differences in characteristics such as hardness, surface shape, water content, etc., especially for fruits of different ripeness. We collected the triboelectric-inductive signals of an unripe banana, half-ripe banana, ripe banana and an overripe banana (Fig. S9a), and reconstructed another dataset by combining the new data with the original data (shown in Fig. 4). Using the same machine learning model, the recognition accuracy of the 11 samples reached 96.82% (Fig. S9b). This result demonstrates that the hybrid sensor system can differentiate the ripeness of fruits.

2.4. Recognition of packaged objects

Sometimes, objects come with package in different forms. Since the triboelectrification only occurs at the interface between the triboelectric sensor and the surface it touches, the triboelectric signal can only reflect the surface property of the package, limiting its ability to perceive the intrinsic property of the object inside the package. However, the electromagnetic induction may penetrate though the package, enabling the inductive sensor to obtain some of the characteristics of the object inside. For example, when an apple is wrapped in a plastic bag, the triboelectric sensor can only reflect the specific charge condition of the plastic bag, which is very different from that of the apple itself (Fig. 5a). On the contrary, the inductive sensor can reflect an electromagnetic characteristic of both the package and the apple inside.

We chose four kinds of fruits wrapped by Paper bag, PVC bag, Foam and nothing to form a total of 16 test samples. Data from 200 gripping of these samples with random grasp settings were collected to construct a new training set. The typical signals from the dual-mode sensor are presented in Fig. 5a-d. After training the CNN model, the confusion matrix exhibits a high recognition accuracy of 95.93% (Fig. 5e), indicating that the fruits inside different packages were effectively identified. In contrast, the recognition accuracy of the fruits inside the packages using triboelectric signals alone is only 63.43% (Fig. S10), which is far lower than the recognition accuracy using the hybrid sensor. The confusion matrix also reveals that the triboelectric characteristics of different fruits in the same package are significantly coupled. Compared with previous works (Table S2), our object recognition method can decouple the interference between the surface material property and electromagnetic induction of the target object, which is a unique comparative advantage.

To characterize the impact of the environmental covariates on object recognition, we conducted an experiment in a controlled environment with preset temperature and humidity (Fig. S11). As shown in Fig. S12a, the triboelectric-inductive signals of four samples (Apple, Orange, Apple wrapped by PVC bag and Orange wrapped by Paper bag) were collected by the hybrid sensor in two temperatures and two humidity levels (18 ℃ & 40% RH and 35 ℃ & 75% RH). The data were mixed with the original 16-sample dataset (24 ℃ & 50% RH). Using the same machine learning strategy, the recognition accuracy of the 16 samples reached 94.375% (Fig. S12b). In comparison with the case where no environment disturbance was taken into consideration, the recognition accuracy drops slightly (from 95.94% to 94.375%). This result indicates that the hybrid sensor and the machine learning model can adapt to environmental variations pretty well. By enriching the training dataset, the recognition accuracy with environment disturbance can further improve.

3. Conclusions

In summary, a triboelectric sensing unit and an inductance transducer were integrated into a hybrid tactile sensor. This hybrid sensor can simultaneously measure the charge interaction properties and the electromagnetic induction characteristics of an object. Equipped with a properly trained machine learning algorithm to process the dual-mode sensing signals, the robotic gripper can successfully identify eight different fruits with an accuracy of 98.75%. The hybrid sensor with the trained machine learning algorithm can also recognize objects inside different packages. The recognition accuracy of four different fruits in three different packages reaches 95.93%. With more precise fabrication technique, the hybrid sensor can achieve better resolution, further improving the aforementioned recognition accuracy. By combining the hybrid tactile sensing system with visual technology, additional improvements in the recognition accuracy can be achieved, which would significantly enhance the functionality of sorting robots.

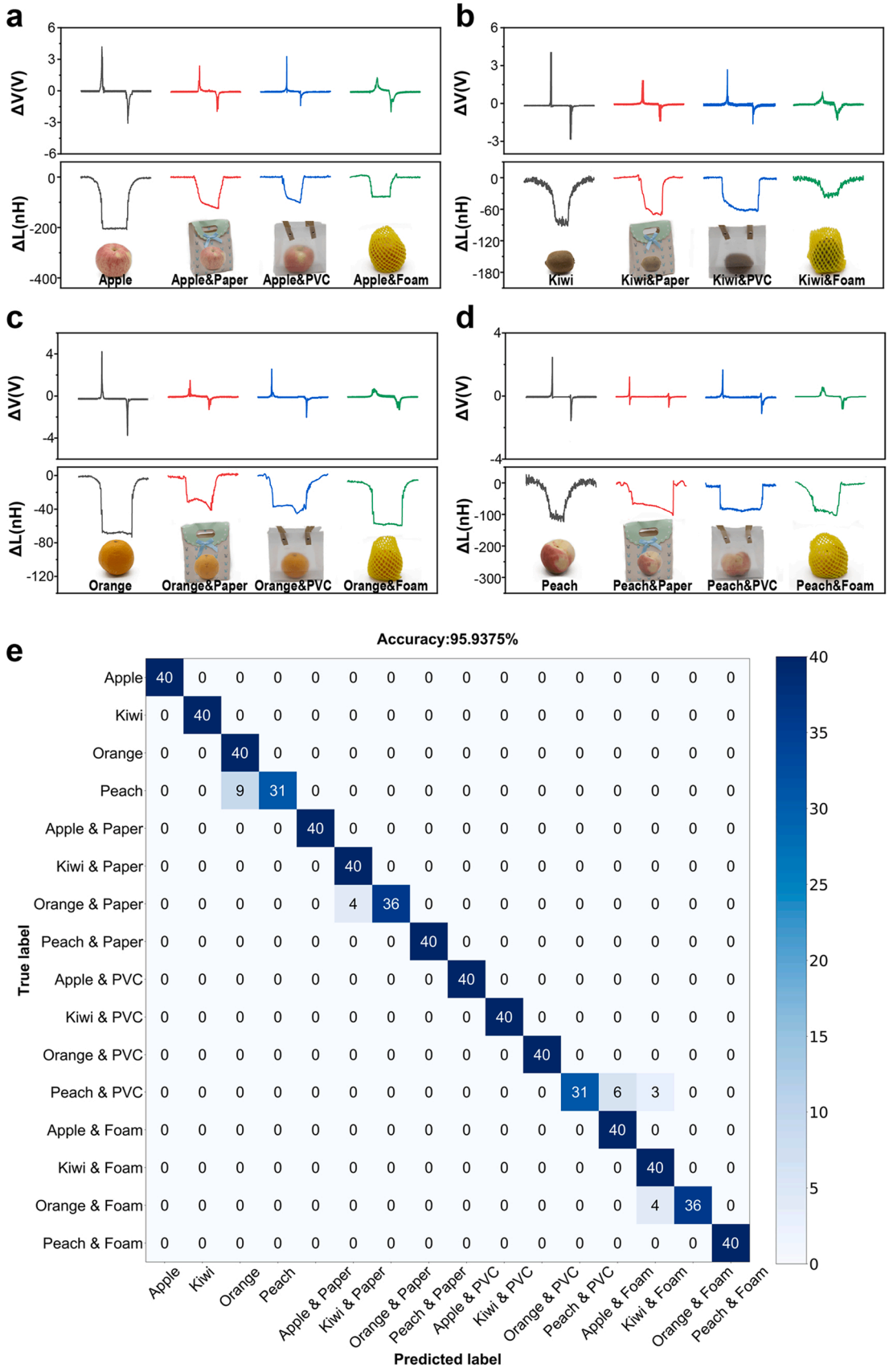

Fig. 5. Packaged item identification by a robotic gripper equipped with the dual-mode hybrid sensor. a-d) Typical waveforms from the dual-mode sensor as the robot grips four kinds of fruits wrapped by a paper bag, a PVC bag, a foam coil and nothing. e) The confusion matrix derived from the CNN model with the database of dual-mode signals.

4. Experimental methods

4.1. Preparation of the device

The electrode of the triboelectric sensor, the spiral coil and shielded wire were fabricated using flexible printed circuit (FPC) manufacture procedure. It starts from a single-sided copper-clad laminate with a polyimide substrate. The width and spacing of the copper coil are both 0.08 mm. Fifty turns of coils were wound to generate a relatively strong magnetic field. The PVDF thin film was laser engraved by a laser machine (Han's laser, GY-ZW-5 W) to fabricate fingerprint-like annular structure on the top surface, and then laminated on the triboelectric electrode.

4.2. Characterization of the device

A universal material test instrument (Instron, E1000) was used to supply the mechanical excitations. The output voltage of the triboelectric sensor was measured using a digital oscilloscope (ZLG, ZDS2024B Plus) with a 10:1 probe. The output signal of the inductive transducer was acquired using an LCR meter (Wayne Kerr, 6500). The waveforms of the bi-signal acquired by the instruments are transferred to a computer and then sliced to build the dataset and loaded into the machine learning model for identification.

The hybrid tactile sensor was then attached to a robotic gripper (Robotiq, 3-Fingers) with a PDMS gasket, the hardness of which is ShoreA-45. The grasping action and applied pressure for holding an object were controlled by a controller. The approaching speed is about 40 mm/s to 48 mm/s. Such speed was chosen to obtain triboelectric signals with relatively high voltage amplitude. As such, the contrast of triboelectric signals for different objects is relatively high. During the training process, we randomly selected the preset grasping programs and assigned them to the controller, and let the gripper grasp each object for several times. During this process, fruits were fed to the gripper in different orientations.

CRediT authorship contribution statement

Ning Li: Conceptualization, Methodology, Investigation, Data curation, Writing – original draft, Writing – review & editing. **Zhuhui Yin:** Investigation, Data curation, Writing – original draft. **Weiguan Zhang:** Supervision. **Chenyang Xing:** Investigation. **Taijiang Peng:** Supervision. **Bo Meng:** Methodology, Investigation, Writing – review & editing. **Jun Yang:** Supervision. **Zhengchun Peng:** Methodology, Supervision, Writing – review & editing.

Declaration of Competing Interest

The authors declare that they have no known competing financial interests or personal relationships that could have appeared to influence the work reported in this paper.

Acknowledgments

This work was supported in part by the Science and Technology Innovation Commission of Shenzhen (Grant Nos. JCYJ20180305124942832, JCYJ20170818091233245, KQTD20170810105439418), in part by the Joint funding program of Guangdong Department of Science and Technology and Hongkong Innovation and Technology Fund (Grant No. 2021A0505110015), in part by National Natural Science Foundation of China (Grand Nos. 61903259, 61904111, 61904112) and Natural Science Foundation of Guangdong Province (Grand No. 2020A1515011487).

Appendix A. Supporting information

Supplementary data associated with this article can be found in the online version at doi:10.1016/j.nanoen.2022.107063.

References

[1] S. Lee, Q. Shi, C. Lee, From flexible electronics technology in the era of IoT and artificial intelligence toward future implanted body sensor networks, APL Mater. 7 (2019), 031302.
[2] D. Kim, B.B. Kang, K.B. Kim, H. Choi, J. Ha, K.J. Cho, S. Jo, Eyes are faster than hands: a soft wearable robot learns user intention from the egocentric view, Sci. Robot 4 (2019) eaav2949.
[3] H. Liu, L. Wang, Gesture recognition for human-robot collaboration: a review, Int. J. Ind. Ergon. 68 (2018) 355–367.
[4] Q. Zhang, J. Zuo, T. Yu, Y. Wang, Visual recognition system of cherry picking robot based on Lab color model, IOP Conf. Ser.: Earth Environ. Sci. 100 (2017), 012099.
[5] S.S. Baishya, B. Bäuml, IEEE/RSJ International Conference on Intelligent Robots and Systems (IROS), 2016, IEEE, 2016, pp. 8–15.
[6] S. Sundaram, P. Kellnhofer, Y. Li, J.Y. Zhu, A. Torralba, W. Matusik, Learning the signatures of the human grasp using a scalable tactile glove, Nature 569 (2019) 698–702.
[7] L. Schein, Applied physics. recent progress and continuing puzzles in electrostatics, Science 316 (2007) 1572–1573.
[8] F. Fan, Z. Tian, Z.L. Wang, Flexible triboelectric generator, Nano Energy 1 (2012) 328–334.
[9] C. Wu, A.C. Wang, W. Ding, H. Guo, Z.L. Wang, Triboelectric nanogenerator: a foundation of the energy for the new era, Adv. Energy Mater. 9 (2019), 1802906.
[10] S. Wang, L. Lin, Z.L. Wang, Triboelectric nanogenerators as self-powered active sensors, Nano Energy 11 (2015) 436–462.
[11] Y. Zi, S. Niu, J. Wang, Z. Wen, W. Tang, Z.L. Wang, Standards and figure-of-merits for quantifying the performance of triboelectric nanogenerators, Nat. Commun. 6 (2015) 8376.
[12] W. Tang, T. Jiang, F.R. Fan, A.F. Yu, C. Zhang, X. Cao, Z.L. Wang, Liquid-metal electrode for high-performance triboelectric nanogenerator at an instantaneous energy conversion efficiency of 70.6, Adv. Funct. Mater. 25 (2015) 3718–3725.
[13] L. Cheng, Q. Xu, Y. Zheng, X. Jia, Y. Qin, A self-improving triboelectric nanogenerator with improved charge density and increased charge accumulation speed, Nat. Commun. 9 (2018) 3773.
[14] H. Guo, X. Pu, J. Chen, Y. Meng, M.-H. Yeh, G. Liu, Q. Tang, B. Chen, D. Liu, S. Qi, C. Wu, C. Hu, J. Wang, Z.L. Wang, A highly sensitive, self-powered triboelectric auditory sensor for social robotics and hearing aids, Sci. Robot. 3 (2018) eaat2516.
[15] J. Zou, M. Zhang, J. Huang, J. Bian, Y. Jie, M. Willander, X. Cao, N. Wang, Z. L. Wang, Coupled supercapacitor and triboelectric nanogenerator boost biomimetic pressure sensor, Adv. Energy Mater. 8 (2018), 1702671.
[16] H. Yang, Y. Pang, T. Bu, W. Liu, J. Luo, D. Jiang, C. Zhang, Z.L. Wang, Triboelectric micromotors actuated by ultralow frequency mechanical stimuli, Nat. Commun. 10 (2019) 2309.
[17] R. Hinchet, H.J. Yoon, H. Ryu, M.K. Kim, E.K. Choi, D.S. Kim, S.-W. Kim, Transcutaneous ultrasound energy harvesting using capacitive triboelectric technology, Science 365 (2019) 491–494.
[18] S. Li, Y. Fan, H. Chen, J. Nie, Y. Liang, X. Tao, J. Zhang, X. Chen, E. Fu, Z.L. Wang, Manipulating the triboelectric surface charge density of polymers by low-energy helium ion irradiation/implantation, Energy Environ. Sci. 13 (2020) 896–907.
[19] H. Wang, L. Xu, Y. Bai, Z.L. Wang, Pumping up the charge density of a triboelectric nanogenerator by charge-shuttling, Nat. Commun. 11 (2020) 4203.
[20] Y. Yang, H. Zhang, J. Chen, Q. Jing, Y.S. Zhou, X. Wen, Z.L. Wang, Single-electrode-based sliding triboelectric nanogenerator for self-powered displacement vector sensor system, ACS Nano 7 (2013) 7342–7351.
[21] B. Meng, W. Tang, Z.H. Too, X. Zhang, M. Han, W. Liu, H. Zhang, A transparent single-friction-surface triboelectric generator and self-powered touch sensor, Energy Environ. Sci. 6 (2013) 3235.
[22] H. Zou, Y. Zhang, L. Guo, P. Wang, X. He, G. Dai, H. Zheng, C. Chen, A.C. Wang, C. Xu, Z.L. Wang, Double-slit photoelectron interference in strong-field ionization of the neon dimer, Nat. Commun. 10 (2019) 1–9.
[23] M. Zhu, Z. Sun, Z. Zhang, Q. Shi, T. He, H. Liu, T. Chen, C. Lee, Haptic-feedback smart glove as a creative human-machine interface (HMI) for virtual/augmented reality applications, Sci. Adv. 6 (2020) eaaz8693.
[24] F. Wen, Z. Sun, T. He, Q. Shi, M. Zhu, Z. Zhang, L. Li, T. Zhang, C. Lee, Machine learning glove using self-powered conductive superhydrophobic triboelectric textile for gesture recognition in VR/AR applications, Adv. Sci. 7 (2020), 2000261.
[25] T. Jin, Z. Sun, L. Li, Q. Zhang, M. Zhu, Z. Zhang, G. Yuan, T. Chen, Y. Tian, X. Hou, C. Lee, U1 snRNP regulates cancer cell migration and invasion in vitro, Nat. Commun. 11 (2020) 1–12.
[26] Z. Sun, M. Zhu, Z. Zhang, Z. Chen, Q. Shi, X. Shan, R.C.H. Yeow, C. Lee, Artificial Intelligence of Things (AIoT) Enabled Virtual Shop Applications Using Self-Powered Sensor Enhanced Soft Robotic Manipulator, Adv. Sci. 8 (2021), 2100230.
[27] Z. Ma, B. Meng, Z. Wang, C. Yuan, Z. Liu, W. Zhang, Z. Peng, A triboelectric-piezoresistive hybrid sensor for precisely distinguishing transient processes in mechanical stimuli, Nano Energy 78 (2020), 105216.
[28] Y. Wang, H. Wu, L. Xu, H. Zhang, Y. Yang, Z.L. Wang, Hierarchically patterned self-powered sensors for multifunctional tactile sensing, Sci. Adv. 6 (2020) eabb9083.
[29] S. Pyo, J. Lee, K. Bae, S. Sim, J. Kim, Recent progress in flexible tactile sensors for human-interactive systems: from sensors to advanced applications, Adv. Mater. 33 (2021), 2005902.
[30] X. Wang, M. Que, M. Chen, X. Han, X. Li, C. Pan, Z.L. Wang, Full dynamic-range pressure sensor matrix based on optical and electrical dual-mode sensing, Adv. Mater. 29 (2017), 1605817.

[31] H. Chen, L. Miao, Z. Su, Y. Song, M. Han, X. Chen, X. Cheng, D. Chen, H. Zhang, Fingertip-inspired electronic skin based on triboelectric sliding sensing and porous piezoresistive pressure detection, Nano Energy 40 (2017) 65–72.
[32] W. Zhang, P. Wang, K. Sun, C. Wang, D. Diao, Intelligently detecting and identifying liquids leakage combining triboelectric nanogenerator based self-powered sensor with machine learning, Nano Energy 56 (2019) 277–285.
[33] G. Li, S. Liu, L. Wang, R. Zhu, Skin-inspired quadruple tactile sensors integrated on a robot hand enable object recognition, Sci. Robot. 5 (2020) eabc8134.
[34] A. Krizhevsky, I. Sutskever, G.E. Hinton, Adv. Neural Inf. Process. Syst. 25 (2012) 1097–1105.
[35] K. Simonyan, A. Zisserman, arXiv preprint arXiv 2014, 1409.1556.
[36] C. Szegedy, W. Liu, Y. Jia, P. Sermanet, S. Reed, D. Anguelov, D. Erhan, V. Vanhoucke, A. Rabinovich, Proceedings of the IEEE Conference on Computer Vision and Pattern Recognition 2015, 1–9.
[37] X. Ying, J. Phys. Conf. Ser. 2 (2019), 022022.
[38] X. Rong, J. Zhao, H. Guo, G. Zhen, J. Yu, C. Zhang, G. Dong, Material recognition sensor array by electrostatic induction and triboelectric effects, Adv. Mater. Technol. 5 (2020), 2000641.

Dr. Ning Li received his Ph.D. degree in communication and information system from the Southwest Jiaotong University in 2017. Currently, he is an associate research fellow at Shenzhen University. His main research interests focus on the fields of flexible & stretchable electronics, tactile intelligent and intelligent recognition strategy based on multi-parameter haptics.

Zhuhui Yin received his Master's Degree from Shenzhen University in 2021. He is currently a research assistant at Shenzhen University. His research interests focus on multi-parameter tactile sensor and the application of sensory system.

Dr. Weiguan Zhang received his Ph.D. degree in electronic engineering from the City University of Hong Kong in 2014. Currently, he is an associate research fellow at Shenzhen University. His research interests include microsensors and flexible electronics.

Dr. Chenyang Xing is currently an assistant professor in College of Physics and Optoelectronic Engineering at Shenzhen University. He received his Ph.D. in Inorganic Chemistry from Shanghai Institute of Applied Physics, Chinese Academy of Sciences in 2016. Dr Xing's research interests include design, manufacturing, and integration of 2D nanomaterials for applications in biomedical application, energy, optoelectronics, and wearable devices.

Taijiang Peng. He received the B.E., M.E., and Ph.D. degrees from the Jilin University, Changchun, China, in 2000, 2003, and 2006, respectively. He is currently an associate professor in the College of Mechatronics and Control Engineering, Shenzhen University. His research interests include intelligent manufacturing, energy harvesting, piezoelectric actuation, IoT, 3D printing, and robotics.

Dr. Bo Meng is currently an assistant professor at Shenzhen University. He received his Ph.D. degree in Microelectronics and Solid-State Electronics from Peking University in 2016. His research interest mainly focuses on micro systems and flexible electronics, especially the applications in energy harvesting and active sensing use.

Jun Yang, Ph.D., P.Eng., FCAE Professor at Shenzhen Institute of Advanced Study, University of Electronic Science and Technology of China. His research interests include Additive Manufacturing/3D Printing, Micro/Nanofabrication, and AI-based and Internet-based Intelligent Manufacturing, Bio-MEMS/MEMS/NEMS, Industrial Internet/Internet of Things, Flexible/wearable Electronics, Biophysics, Lab-on-a-chip and biotechnology, etc.

Dr. Zhengchun Peng received his Ph.D. degree (2010) in MEMS from the Georgia Institute of Technology. He then joined Intel as a senior R&D engineer. He is currently a distinguished professor at Shenzhen University since 2015. His main research interests focus on the fields of flexible & stretchable electronics, bio-MEMS & microfluidics, and tactile intelligent.